Published in final edited form as:
Pain. 2007 May ; 129(1-2): 76–92.

Immunohistochemical Localization of Histamine H_3 Receptors in Rodent Skin, Dorsal Root Ganglia, Superior Cervical Ganglia and Spinal Cord: Potential Antinociceptive Targets

Keri E. Cannon[1], **Paul L. Chazot**[2], **Victoria Hann**[2], **Fiona Shenton**[2], **Lindsay B. Hough**[1], and **Frank L. Rice**[1,*]

1 *Center for Neuropharmacology and Neuroscience, Albany Medical College MC-136, Albany, NY, USA*

2 *School of Biological and Biomedical Sciences, University of Durham, Durham, UK*

Abstract

Activation of histamine H_3 receptors (H_3Rs) reduces inflammation and nociception, but the existence of H_3Rs on peripheral innervation has never been demonstrated. Here we use antibodies to locate H_3Rs in whisker pads, hairy and glabrous hind paw skin, dorsal root ganglia (DRGs), and spinal cords of rats, wild-type mice, and H_3R knockout (H_3KO) mice. Although H_3Rs have been hypothesized to be on C and sympathetic fibers, H_3R-like immunoreactivity (H_3R-LI) was only detected on presumptive periarterial Aδ fibers and on Aβ fibers that terminated in Meissner's corpuscles and as lanceolate endings around hair follicles. The H_3R-positive periarterial fibers were thin-caliber and coexpressed immunoreactivity for calcitonin gene-related peptide (CGRP), substance P, acid sensing ion channel 3 and 200kD neurofilament protein (NF). H_3R–LI was also detected on epidermal keratinocytes and Merkel cells, but not on Merkel endings, C fibers, any other Aδ fibers, or sympathetic fibers. In DRGs, H_3R-LI was preponderantly on medium to large neurons coexpressing NF-LI and mostly CGRP-LI. In dorsal horn, CGRP-positive fibers with and without H_3R-LI ramified extensively in lamina II; many of the former formed a plexus in lamina V. Low levels of H_3R-LI were also present on Aβ fibers penetrating superficial and into deeper laminae. The distribution of H_3R-LI was similar in rats and wild-type mice, but was eliminated or strongly reduced in Aδ fibers and Aβ fibers, respectively, in H_3KO mice. Taken with recently published behavioral results, the present findings suggest that periarterial, peptidergic, H_3R-containing Aδ fibers may be sources of high threshold mechanical nociception.

Keywords

histamine; H_3 receptors; arterial innervation; Aδ fibers; Aβ fibers; calcitonin gene-related peptide; substance P; sensory innervation

INTRODUCTION

Histamine is a chemical messenger that is released by neuronal and non-neuronal sources (Hough and Leurs, 2006). Histamine can act at four known types of histamine receptors,

*Corresponding author: Dr. Frank L. Rice, Center for Neuropharmacology and Neuroscience, Albany Medical College, 47 New Scotland Avenue, Albany, NY 12208, E-mail: ricef@mail.amc.edu

including H_3 receptors (Hough, 2001). Although H_3 receptors (H_3Rs) were originally reported to exist in the CNS as presynaptic inhibitory autoreceptors (Arrang et al., 1983;Arrang et al., 1987), lesion studies have revealed that a large fraction of brain H_3Rs exist as postsynaptic inhibitory heteroreceptors (Pollard et al., 1993). Subsequently, pre- and postsynaptic expression of H_3Rs has been detected throughout the CNS. Detailed H_3R radioligand binding in rat brains revealed high densities of binding sites in the cerebral cortex, striatum, and olfactory tubercles (Pollard et al., 1993). In agreement with this distribution, *in situ* hybridization studies showed strong H_3R mRNA signals in the cerebral cortex, thalamus, and striatum of the rat (Lovenberg et al., 1999;Drutel et al., 2001). Although the majority of H_3Rs are located in the brain, H_3R mRNA is also found in various non-brain tissues, including skin, dorsal root ganglia, stomach, intestines, and brown adipose tissue (Heron et al., 2001;Karlstedt et al., 2003).

Administration of H_3R agonists has been shown to inhibit neuropeptide release from sensory fibers in the heart, lung, and skin, leading to the hypothesis that H_3Rs are located on peptidergic C fibers (Dimitriadou et al., 1994;Ohkubo et al., 1995;Delaunois et al., 1995;Imamura et al., 1996;Dimitriadou et al., 1997;Nemmar et al., 1999). Consistent with this hypothesis, recent studies revealed that H_3R agonists have anti-inflammatory as well as some antinociceptive properties (Rouleau et al., 1997;Rouleau et al., 2000;Cannon et al., 2003;Cannon and Hough, 2005). Other studies suggest that H_3Rs are located on sympathetic efferents (Ishikawa and Sperelakis, 1987;Molderings et al., 1992;Koss, 1994;Godlewski et al., 1997a;Godlewski et al., 1997b). However, no immunohistochemical studies have been performed to determine the precise localization H_3Rs on either sensory or sympathetic fibers. Thus, the present study has performed the first investigation of the distribution of H_3R immunofluorescence on nerve cells and fibers in skin, dorsal root ganglia, and spinal cords of rats and mice.

MATERIALS AND METHODS

Specimens

The subjects were 6 rats, 6 wild type mice, and 6 H_3KO mice. Animal housing and procedures were approved by the Institutional Animal Care and Use Committee of Albany Medical College. Male Sprague-Dawley rats (300–350 g, Taconic Farms, Germantown, NY), housed in groups of two or three per cage, and female wild type or H_3KO mice (10–14 weeks old, 20–30 g), housed up to seven per cage, were maintained on a 12 h light/dark cycle (lights on from 7:00 to 19:00 h). Food and water were provided *ad libitum*.

H_3KO mice, kindly provided by Millennium Pharmaceuticals, Inc. (Cambridge, MA), were generated by targeted deletion of exon 3 of the mouse H_3R gene (Cannon et al., 2003). H_3KO mice showed no detectable histamine H_3R mRNA in the brain or the spinal cord by *in situ* hybridization (Cannon et al., 2003). Brains from these subjects also had no detectable histamine H_3R binding (Mobarakeh et al., 2003). Following an overdose of sodium pentobarbital, the animals were transcardially perfused with 0.9% saline, followed by 4% paraformaldehyde in 0.1M phosphate-buffered saline (PBS, pH 7.4, 4°C). Immediately after perfusion, the tissues were dissected and post-fixed at 4°C in perfusion fixative for 4 hours. Following post-fixation, the tissues were rinsed several times in PBS and stored in 0.1% sodium azide PBS. The following tissues were taken from each animal: 1) lumbar spinal cord, 2) lumbar dorsal root ganglia (DRG), 3) superior cervical ganglia (SCG), 4) glabrous and hairy skin from hind paws, and 5) whisker pads. The forebrains were removed from some rats, wild type mice and H_3KO mice for control purposes.

For cryostat sectioning, tissues were cryoprotected by overnight immersion in PBS containing 30% sucrose at 4ºC. Serial sections (14μm-thick) were cut on a cryostat and thawed in

sequential order onto and rotating across 5–15 gelatinized slides. The slides were air dried overnight and processed for single or double immunolabeling.

Production and characterization of H_3R antibodies

Our study used two different rabbit polyclonal antibodies for H_3R: one produced by Chazot et al. (2001) and the other obtained commercially (AB5660P, Chemicon, see Table 1). The Chazot antibody was directed against residues 349–358 of the human and rat H_3R, which is identical in the mouse sequence. Western blots on P2 membranes taken from wild type and H_3KO forebrains were performed with this antibody as previously described (Chazot et al., 2001). Proteins (30 μg) were extracted using the chloroform/methanol precipitation method, and the precipitate subjected to SDS-PAGE under reducing conditions, using 7.5% (v/v) acrylamide slab gels. Proteins were transferred onto nitrocellulose, probed with the H_3R antibody (2 μg/ml), and detected using an ECL PLUS system (Amersham, UK). The Chemicon antibody was targeted against an 18 amino acid sequence in the C-terminus region of rat H_3R. This sequence is 100% identical in mouse, 88% conserved in guinea pig, and 82% in human H_3R.

Immunofluorescence preparation and observation

As previously described (Rice et al., 1997;Pare et al., 2002), serial 14μm sections were prepared for single or double labeling with the antibodies listed in Table 1. Antibodies were diluted in a PBS solution containing 1% bovine serum albumin (BSA) and 0.3% Triton X-100. Appropriate species of secondary antibodies were raised in donkey or goat and conjugated with either Cy3 (1:250; Jackson ImmunoResearch Laboratories, Inc.), Cy2 (1:500; Jackson ImmunoResearch Laboratories, Inc.), or Alexa 488 (1:500; Molecular Probes, Inc.).

Slides were first preincubated in PBS containing 1% BSA and 0.3% Triton X-100 for 30 minutes, then incubated overnight at 4ºC in primary antibody under high humidity. Following a 30 min rinse in PBS, slides were incubated under the appropriate secondary antibody for 2 hours at room temperature then rinsed for 30 min in PBS. For double labeling, the sequence was repeated with the desired additional primary antibody and its appropriate secondary antibody. After the final rinse, slides were coverslipped with 90% glycerin/10% PBS solution. If the two primary antibodies were raised in different species, then the double labeling revealed by Cy3 and Cy2 (or Alexa 488) was clearly separate. In some cases, double labeling combinations were desired where only two rabbit primary antibodies (A and B) were available or optimal. After verifying that separate single labeled preparations with each antibody labeled similar innervation in a specific anatomical location, some slides were incubated first with antibody A followed by anti-rabbit Cy3, then incubated with antibody B followed by anti-rabbit Cy2 or Alexa 488. Other slides with alternating tissue sections were processed with the sequence of primary antibodies reversed (i.e., first B, then A). The validity and limitations of this double labeling method have been discussed in detail (Rice et al. 1997). For example, if fibers and endings labeled with A are a subset of those labeled with B, then the first sequence will have some fibers and endings that will be double labeled both with Cy3 and Cy2, whereas additional fibers and endings will only be labeled with Cy2. In the reverse sequence, all fibers and endings will be double labeled, and none will be only labeled with Cy2.

Immunochemical specificity and fiber classification

As shown in previous studies, protein gene product 9.5 (PGP) is a pan-neuronal cytoplasmic enzyme (Rice et al., 1997). As such, anti-PGP labels all types of normal cutaneous innervation in rats and mice including sympathetic fibers and various types of sensory fibers (i.e. Aβ, Aδ and C fibers), as well as their terminations (Rice et al., 1997;1998;Fundin et al., 1997a,b;Fünfschilling et al., 2004;Zylka et al., 2005). Other antibodies directed against 200kD neurofilament (NF), CGRP, substance P (SP) and neuropeptide Y (NPY) discriminate between specific types of innervation. The previous studies on rat skin cited above demonstrated that

NF-LI was present on all thick-caliber and many thin-caliber sensory fibers. The anti-NF labeling in the rat was consistently coexpressed with myelin basic protein (MBP) LI indicating that these thick and thin fibers are Aβ and Aδ fibers respectively. NF-positive fibers with thick and thin calibers that have similar distributions and types of endings are also present in mouse skin. Based upon their morphologically distinct endings, the thick caliber fibers are the clear equivalent of the Aβ fibers in the rat. The thin NF-positive caliber fibers in the mouse are presumably the equivalent Aδ fibers, although in attempting to directly confirm this presumption we haven't found an antibody that effectively reveals myelin basic protein in sections of mouse skin. CGRP-LI and SP-LI are vasodilatory neuropeptides commonly coexpressed in subsets of Aδ and C "peptidergic" fibers in mouse and rat skin. Likewise, in mouse and rat skin, NPY is a neuropeptide normally expressed mostly in adrenergic sympathetic fibers that also are immunoreactive for tyrosine hydroxylase and are implicated in vasoconstriction.

Three experiments were performed to control for nonspecific labeling. First, incubations were conducted without the primary antibody to observe immunofluorescence provided by the secondary antibody alone. Second, slides were incubated under primary antibodies that had been preincubated with their specific blocking peptide to observe any nonspecific interactions of the primary antibody. Blocking peptide was added to the H_3R antibody at 1000-fold molar excess and was allowed to sit at room temperature for one hour prior to application to tissue sections. Third, immunolabeling was assessed in H_3KO mice. To recognize the possibility that an antibody made against a particular antigen might label a different, albeit antigenically similar molecule, all detectable immunofluorescence will be referred to as a particular antigen-like immunoreactivity (LI), for example H_3R-LI. For simplicity, structures having LI for a particular antigen will also be referred to as positive for that antigen, for example H_3R–positive.

Sections were analyzed with an Olympus Provis AX70 microscope equipped with conventional fluorescence: 1) Cy3 filters (528–553 nm excitation, 590–650 nm emission), and 2) Cy2 filters (460–500 nm excitation, 510–560 nm emission). Fluorescence images were captured with a high resolution (1280 × 1024 pixels) three chip color CCD camera (Sony, DKC-ST5) interfaced with Northern Eclipse software (Empix Imaging, Inc., Mississauga, ON).

Since the intensity of immunolabeling for the numerous antibodies used in the present study is attributed to many variables that cannot be individually quantified, this study does not attempt to quantify the relative amounts of labeled antigens. These variables include: 1) true differences in the presence and quantity of the antigen, 2) whether the antibody is monoclonal or polyclonal, 3), background labeling, 4) antibody concentration, 5) efficacy of the antibody, and 6) location of the antigen (i.e. membrane or cytosol). Because the labeling intensities differed between the various types of antibodies, the photomicrographs compiled for illustrative purposes were adjusted using Northern Eclipse, Adobe Photoshop (San Jose, CA), and Microsoft Powerpoint (Redmond, WA) software so that the maximum labeling contrast and intensity were similar for each antibody.

Dorsal root ganglia quantifications

Analyses of the double labeling combinations in DRGs and SCGs were performed with Neurolucida software (MicroBrightField, Inc., Willston, VT). Analyses were conducted for sections spaced at least 100μm apart from three L4 or L5 DRGs double-labeled with antibodies for 1) H_3R and calcitonin gene-related peptide (CGRP), 2) H_3R and substance P (SP) and 3) for H_3R and 200kD neurofilament protein (NF). The H_3R and CGRP antibodies were raised in rabbit and guinea pig (respectively), allowing for distinct detection of single or double labeling. The H_3R and NF antibodies were both made in rabbit. Single labeling with anti-H_3R or anti-NF revealed that many neurons expressed H_3R-LI and/or NF-LI. Sequential incubations first with anti-H_3R followed by anti-rabbit Cy3, then in anti-NF followed by anti-

rabbit Cy2 revealed that many neurons had NF-LI without H_3R-LI. Sequential incubations first with anti-NF followed by anti-rabbit Cy3, then anti-H_3R followed by anti-rabbit Cy2 revealed that virtually all the anti-H_3R labeled neurons coexpress NF-LI. Interestingly, since anti-H_3R labeling was much less robust than anti-NF labeling, when H_3R antibodies were used first in the double labeling sequence the subsequent binding of the first anti-rabbit secondary antibody effectively blocked any erroneous cross labeling by the anti-rabbit secondary antibody used in the second round of incubations.

In order to standardize assessment of labeling, digital images of double labeled ganglion sections were captured separately for the red (Cy3) and green (Cy2 or Alexa 488) fluorescent channels, using camera settings that produced a comparable range of low fluorescence intensities in each channel. The lowest fluorescence intensities captured for each antibody were set to levels comparable to the fluorescence captured from sections processed only with the secondary antibodies. Next, the range of fluorescence intensities in each channel was adjusted linearly so that many cells remained barely evident, and the most brightly fluorescing cells had a comparable intensity in both channels. The resultant images in the red and green channels were merged by Boolean addition and the double labeled images were stored. A copy of each double labeled image was purposefully extremely enhanced so that contours of even the most faint cell profiles in the background could be delineated. Using these extremely enhanced images, the contours of all visible cells were circumscribed to calculate the area of each cell for as many cells as possible. The contour outlines obtained in the enhance images were then superimposed onto separate copies of the unenhanced red and green images. In each channel, the labeling of the cell underlying each contour was subjectively rated as: 1) blank, 2) very weak, 3) weak, 4) moderate or 5) strong. The independent results from each channel were then combined to conclude which cells had labeling for either or both antibodies. Only those cells regarded as weak, moderate, or strong in each channel were regarded as “labeled” for the antibody corresponding to the particular channel. The Abercrombie correction (1946) was used to compensate for the progressive under representation of cells that occurs in proportion to decreasing diameter.

RESULTS

Characterization of the H_3R antibody

In order to more fully characterize the H_3R antibody first developed by Chazot et al. (2001), this antibody was used to detect H_3R-LI in coronal brain sections of rats, wild type mice and H_3KO mice. In rats and wild type mice, pronounced H_3R-LI was observed in several brain regions known to contain moderate to high levels of H_3R mRNA in rats (Pollard et al., 1993;Heron et al., 2001;Pillot et al., 2002). For example, in both species we found robust H_3R-LI in the striatum (Fig. 1A), consistent with the previous detection in rats of H_3R mRNA in the striatum and H_3R-LI on striatal, medium spiny neurons of rats. H_3R-LI was also observed in the cingulate cortex, substantia nigra pars reticulata, and cerebral cortex of rats and wild type mice (data not shown). In contrast, the medial septal regions and hippocampal pyramidal layers of rats and wild type mice contained little to no H_3R-LI (data not shown), consistent with the published paucity of H_3R mRNAs in these locations (Pollard et al., 1993;Heron et al., 2001;Pillot et al., 2002). Analysis of brain sections taken from H_3KO mice revealed a virtually complete absence of H_3R-LI in most brain regions examined, including the striatum (Fig. 1C). However, a weak residual H_3R-LI remained in the cerebral cortex and cingulate cortex of H_3KO mice (data not shown).

In Western blots performed on membrane extracts from the forebrains of wild type mice (Fig. 1D), two major H_3R-related species were detected (M_r 93,000 and M_r 68,000), as previously seen in the rat (Chazot el al., 2001). These immunoreactive species were eliminated in H_3KO forebrain extracts (Fig. 1D). The two species are likely to represent dimeric mouse H_3R

isoforms as has been suggested using cross-linking strategies (Shenton et al., 2005). A third, previously unknown species (M_r 95,000) was faintly labeled in wild type extracts and persisted at lower levels in H_3KO extracts (Fig. 1D), which might account for weak residual immunolabeling in H_3KO tissues. The residual labeling may be due to an H_3R-like protein or protein fragment, or to a protein completely unrelated to H_3Rs. However, a Genbank BLASTp search of the H_3R antibody peptide sequence revealed no similarities to any other known vertebrate protein. Although several H_3R isoforms have been proposed to exist (Coge et al., 2001;Wellendorph et al., 2002;Drutel et al., 2001;Tardivel-Lacombe et al., 2000;Rouleau et al., 2004), the H_3KO gene construct eliminated the sequences encoding the epitopes used to make both of the H_3R antibodies.

In other control experiments, brain sections as well as hind paw and whisker pad skin sections from rats, wild type mice, and H_3KO mice were examined after incubation with H_3R antibody serum that had undergone preabsorption with the specific blocking peptide. The preabsorbed serum failed to label any components in all three types of animals (e.g. Fig. 2J–L). Finally, immunofluorescence studies of brain, skin, and spinal cord were repeated in rats, wild type mice, and H_3KO mice using a commercially-available H_3R antibody (see Table 1) that targeted a different portion (C-terminus) of the H_3R protein sequence. In all cases, results with the commercially-available H_3R antibody yielded comparable H_3R-LI patterns in rat, wild type mouse and H_3KO mouse tissues similar to the labeling patterns observed with the Chazot anti-H_3R (e.g. Figs. 1B, 4A–C). However, the Chazot antibody produced consistently more robust labeling and was used for most of the double labeling analyses (e.g. compare Figs. 3A–C and Figs. 4A–C).

Anti-H_3R labeling in skin

In order to determine specifically which types of cutaneous innervation express H_3Rs, sections of glabrous and hairy hind paw skin and of whisker pad skin from rats, wild type mice and H_3KO mice were processed for immunofluorescence with the two H_3R antibodies in combinations with antibodies for several other neuronal antigens (Table 1). As expected, anti-PGP labeled all types of previously known sensory and sympathetic innervation in our skin specimens, including all the types labeled with the other antibodies. The anti-PGP-labeled innervation consisted of numerous thin-caliber fibers that ramify and terminate as free nerve endings (FNEs) in the epidermis and superficial dermis (Fig. 2). Virtually all of the thin-caliber epidermal and superficial dermal innervation lacked H_3R-LI in rats and wild type mice (Fig. 2A–F). This included all combinations of CGRP, SP and NF-positive and negative fibers indicative of peptidergic and nonpeptidergic Aδ and C fibers. Surprisingly, H_3R-LI was detected on thick-caliber Aβ fibers that terminated as lanceolate endings around hair and whisker follicles and as endings in Meissner corpuscles located in the dermal papillae of glabrous skin (Figs. 2A–F; D–F inset). Likewise, the H_3R antibodies labeled the more proximal portions of these Aβ fibers passing through large nerves in the deep dermis (Figs. 3, 4). As has been published previously, all of the Aβ fibers labeled with anti-NF (not shown). H_3R-LI was also detected on Merkel cells located in lamina basalis of the glabrous epidermis and in the outer root sheath of whisker follicles (Figs. 2D–F), but H_3R-LI was not definitively evident on the Aβ fibers that innervate the Merkel cells. Finally, H_3R-LI was detected on keratinocytes of the epidermis, with the strongest expression in the stratum granulosum and stratum spinosum (Figs. 2A–F). Anti-H_3R labeling in H_3KO mice was severely reduced but faint labeling persisted on the Aβ fibers, Merkel cells and keratinocytes (Figs. 2G–I).

Although the H_3R antibodies failed to label thin-caliber fibers of the epidermis and upper dermis, H_3R-LI was detectable on a subset of thin-caliber fibers affiliated with arteries and arterioles deep in the dermis of rats (Figs. 3A–C) and mice (Figs. 3D–F). However, unlike the

faint residual labeling on Aβ fibers, H_3R-LI was completely absent on these deep dermal, periarterial fibers of H_3KO mice (Figs. 3G–I).

Next we sought to determine the identity of these fibers. Previous studies in rats and mice demonstrated that the cutaneous periarterial innervation consists of thin-caliber sensory and sympathetic fibers (Fundin et al., 1997b;Fünfschilling et al. 2004). In the rat, all of the sensory innervation labels with anti-CGRP and anti-SP. Some of it also labels with anti-NF, and anti-MBF, and is presumptively classified as Aδ. The sensory innervation is relatively sparse and is located primarily in the tunica adventitia (Fundin et al., 1997b;Fünfschilling et al. 2004). Other peptidergic periarterial sensory fibers in mouse and rat lacked NF-IR and MBP-IR, indicating that they are C fibers. In contrast to the sensory innervation, virtually all of the normal periarterial sympathetic innervation coexpresses tyrosine hydroxylase and NPY, and distributes as a dense plexus at the border between the tunica adventitia and tunica media. Thus, both the anatomical localization of the innervation, and the immunochemical characteristics of the periarterial innervation permit a clear classification of these fibers as either Aδ, C, or sympathetic.

As seen in our anti-PGP double labeled preparations, virtually all of the anti-H_3R labeled periarterial fibers were located in the tunica adventitia on a subset of fibers within the small vascular nerves and on some of the individual fibers (Figs. 3A–F). Moreover, the anti-H_3R labeled fibers consistently colabeled with anti-CGRP (Figs. 4D–F), anti-SP (Fig. 4G–I) and anti-NF (Fig. 4J–L) indicating that the H_3R-LI was primarily if not exclusively on the presumptive Aδ fiber innervation. The remaining CGRP/SP-positive fibers, which lack NF-LI, were virtually all H_3R-negative indicating that most if not all of the C fibers were H_3R-negative. Although some C fibers could potentially be H_3R–positive, H_3R–LI was never detectable unless some NF-LI was also present. Unfortunately, the H_3R–LI was not sufficiently intense for capture by confocal microscopy at a resolution that was any better than that achieved by epifluorescence, especially since the sections were only 14 μM thick. In a study of vascular innervation in muscle (Molliver et al., 2005), the Aδ vascular fibers were also found to label with antibodies against the acid sensing ion channel 3 (ASIC3). Likewise, we found that the H_3R-positive periarterial fibers also colabeled with anti-ASIC3 in the skin (Figs. 4P–R).

Our double label assessments with anti-PGP revealed very little H_3R-LI among the dense plexus of fibers that ramify at the tunica media and adventitia border. H_3R-LI was especially absent in this location in the rat (Figs. 3A–C), but barely detectable H_3R-LI was present on some fibers in this location in wild type mice (Figs. 3D–F). Double labeling assessments with anti-NPY revealed no co-labeling with H_3R-LI (Figs. 4M–O), thereby supporting the observations indicating that the detectable anti-H_3R labeling was restricted to the Aδ sensory innervation. H_3R-LI was also absent among the sweat glands of the glabrous skin that are the site of dense cholinergic sympathetic terminations (data not shown).

Anti-H_3R labeling in DRG cell bodies

Our immunochemical localization of H_3Rs on some cutaneous innervation was consistent with previously detected moderate levels of H_3R mRNA in DRGs (Heron et al., 2001). However, as noted above, our assessments of cutaneous innervation indicated that H_3R-LI was definitively detectable only on Aβ fibers that terminated as lanceolate endings and Meissner's corpuscles, and on CGRP/SP-positive Aδ fibers that innervate arteries and arterioles. Therefore, our next objective was to assess the size and immunochemical characteristics of neurons in rat lumbar DRGs. Consistent with a general relationship between DRG neuronal diameter and fiber caliber (McCarthy and Lawson, 1990), virtually all neurons less than 25μm in diameter were NF-negative, about 20–30% of neurons from 25 to 35 μm were NF-positive, and virtually all larger neurons were NF-positive (Fig. 6A). Although there are known to be exceptions to this correlation, smaller neurons are typically the source of C fibers and

larger neurons the source of Aβ fibers (McCarthy and Lawson, 1990). Aδ fibers presumably arise mostly from medium sized neurons.

Depending upon whether anti-H_3R treated DRG sections were double labeled with anti-NF or anti-CGRP, a considerable discrepancy was evident between the percentage of total neurons that were initially judged as H_3R-positive: i.e. 33% in section double labeled with anti-NF vs. 55% with anti-CGRP. Presumably the percentage of H_3R-LI neurons should be the same in both types of preparations. An assessment of the overall distribution of all labeled and unlabeled cells revealed that the discrepancy was among the cells less than 25μm in diameter, where a much greater total number of cells regarded as unlabeled were detected in anti-H_3R/anti-NF treated sections than in anti-H_3R/CGRP treated sections. Thus, unlabeled cells were over-represented in the former and/or under-represented in the latter. This may have been due to the potential additive effect of background levels of cross labeling among the primary and secondary antibodies raised in the same species. Based on prior assessments of the proportion of CGRP-positive and negative small cells and of NF-positive and negative small cells in DRGs (e.g. Zylka et al., 2005), it was evident that the discrepancy in small cell counts was primarily due to a lack of overall unlabeled small cell detection in our anti-CGRP labeled specimens. Therefore the graphs in Figure 6B were normalized to the small cell counts in Figure 6A. Independent of the small cell discrepancy, it must be emphasized that H_3R-LI in the DRG was detected primarily on medium to large cells equal to or greater than 25μm in diameter. Among cells of this size, 33–55% are H_3R positive.

In DRG sections taken from H_3KO mice, H_3R-LI was virtually eliminated on the small and medium size neurons, but some weak residual labeling persisted on large neurons (Fig. 5B). Consistent with our peripheral innervation double labeling results, about two-thirds of the neurons with H_3R-LI also coexpressed anti-CGRP labeling (Figs. 5C, D and Figs. 6B, C), and nearly all H_3R-LI cells (97%) co-labeled with anti-NF (Figs. 5G, H and Figs. 6D, E). In comparison to CGRP/H_3R co-localization, about half as many small, medium and large H_3R-positive neurons also coexpressed SP-LI (Fig. 5E, F). This is consistent with previous observations that SP is present in about half of the neurons that contain CGRP (Ju et al., 1987; Lawson et al., 1995), although SP has previously been shown to have nearly complete co-localization with CGRP in cutaneous fibers (Fundin et al., 1997a,b;Rice et al., 1997). At least some of the medium-sized neurons that are positive for CGRP, SP, NF and H_3R (approximately 25–35 μm) may be the source of the vascular Aδ fibers that express the same immunolabeling characteristics. Likewise, the larger-sized neurons (greater than 35 μm) with H_3R-LI may be the source of the H_3R-positive Aβ fibers seen in the skin that supply lanceolate or Meissner endings (Figs. 2D–F). Interestingly, many if not most of the large neurons with H_3R-LI also expressed CGRP and SP-LI. This is consistent with previous observations of low levels of CGRP and SP-LI in lanceolate and Meissner endings, even though the peptide immunoreactivity was usually below detectable levels in their Aβ source axons (Fundin et al., 1997a;Rice et al., 1997; Paré et al., 2001).

A bimodal distribution was observed among H_3R-negative/NF-positive, medium- and large-sized neurons (Fig. 6A). The larger of these neurons may give rise to Aβ fibers that innervate Merkel endings. As noted above, the Merkel cells in the epidermis of the glabrous skin and outer root sheath of whisker follicles expressed H_3R-LI, but this labeling was not definitively evident on the Aβ fibers that form endings on the Merkel cells. The more medium-sized H_3R-negative/NF-positive neurons may be the source of Aδ fibers that have been shown to innervate the epidermis, upper dermis and hair follicles where no anti-H_3R labeling was detected among thin-caliber fibers (Fundin et al., 1997a;Rice et al., 1997;Fünfschilling et al., 2004). Likewise, about one-third of the small- to medium-sized anti-CGRP labeled neurons lacked H_3R-LI (Fig. 6B). These cells may be sources of peptidergic C fibers (some of which terminate on arteries) and non-arterial peptidergic Aδ fibers that also lacked immunodetectable H_3R in the skin

(Fundin et al., 1997a,b;Rice et al., 1997). Regardless of some discrepancy in the detection of unlabeled small neurons in anti-CGRP as compared to anti-NF double labeled section, most small neurons in both types of preparations lacked immunodetectable CGRP, SP, NF or H_3R. This is consistent with the lack of anti-H_3R labeling on any C fibers in the skin of which most are non-peptidergic (Fundin et al., 1997a,b;Rice et al., 1997;Zylka et al., 2005).

Anti-H_3R labeling in superior cervical ganglia

Although many previous functional studies suggested that the H_3R may be located on sympathetic innervation (Ishikawa and Sperelakis, 1987;Molderings et al., 1992;Koss, 1994;Godlewski et al., 1997a;Godlewski et al., 1997b), we rarely detected H_3R-LI on any NPY-positive fibers or on fibers in sites where sympathetic fibers are known to terminate on arteries. Therefore, we assessed anti-H_3R labeling in superior cervical ganglia of rats in double label combination with an antibody against NPY which is widely expressed among adrenergic sympathetic neurons. These results revealed a heterogeneous mix with some neurons coexpressing NPY-LI and H_3R-LI and others expressing only NPY-LI or H_3R-LI (Fig. 5I–J).

Anti-H_3R labeling in dorsal horn

Consistent with the characteristics of H_3R-positive cutaneous fibers, our immunofluorescence assessments of rat and wild type mouse spinal cords revealed H_3R-LI on several thick and thin-caliber axons entering the superficial dorsal horn via dorsal roots (Figs. 7A–L). The thick-caliber, H_3R-LI axons passed through laminae I and II and penetrated at least as far as lamina III in both species (Figs. 7G–I, J–L) Although a few cases were found in which thick-caliber, H_3R-LI axons were also faintly labeled with anti-CGRP, most of the thick-caliber, H_3R-LI axons were CGRP-negative (Figs. 2G–L). In contrast, thin-caliber, H_3R-LI axons consistently co-expressed anti-CGRP labeling (Fig. 7D–L). Many of these thin-caliber fibers ramified extensively in lamina II, and some extended to and ramified in lamina V (Figs. 7D–F, J–L). These observations suggest that the thin-caliber, H_3R-LI fibers synapse on neurons in both locations. Interestingly, CGRP and H_3R-LI was coexpressed on most of the fibers ramifying in lamina V, whereas lamina II also had many CGRP fiber ramifications that lacked H_3R-LI. In general, CGRP-positive fibers that lacked H_3R-LI were thinner than those that expressed H_3R-LI. Superficial (i.e. laminae I-III) dorsal horn neurons appeared to lack H_3R-LI. Sparsely scattered neurons in the deep dorsal horn and ventral horn were faintly labeled with anti H_3R (insert, Fig. 7E) and lacked CGRP-IR making it unlikely that they were the source of any H_3R/CGRP-positive fibers in the dorsal horn. Moreover, the sparsely scattered locations of these neurons did not correlate with the concentrated sites of H_3R-LI fibers in the dorsal horn. In spinal sections from H_3KO mice, H_3R-LI was completely absent on thin-caliber axons in the superficial and deep dorsal horn (Figs. 7M–O). Although the labeling intensity was drastically reduced, faint detectable H_3R-LI was observed in H_3KO mice on thick-caliber afferents found in the lumbar dorsal roots as well as thick-caliber fibers that passed through laminae I-II and entered into laminae III-V (Figs. 7M–O).

DISCUSSION

Functional studies have suggested that H_3Rs exist on sensory peptidergic C-fibers and on sympathetic efferents, but no previous immunochemical experiments have been reported. The present work has not confirmed these suggestions. Results with various combinations of double labeling found that H_3R-LI was detectable only on 1) peptidergic presumptive Aδ fibers that innervate cutaneous arteries and on 2) Aβ fibers that terminate in Meissner corpuscles in glabrous skin and as lanceolate endings in hairy skin. H_3R-LI was also present on epidermal keratinocytes, which contain H_3R mRNA (Heron et al., 2001), as well as on Merkel cells in lamina basalis of the epidermis and the outer root sheath of whisker follicles. All of these H_3R-positive structures contain CGRP-LI. Low levels of this labeling in keratinocytes was

seen previously but disregarded as nonspecific (Rice et al., 19974; Rice and Rasmussen, 2000; Paré et al., 2001; Khodorova et al., 2004; Fünfschilling et al., 2004). H_3R–LI was not definitively evident on 1) peptidergic C fibers, non-peptidergic C fibers, or Aδ fibers that innervate the epidermis or hair follicles; 2) peptidergic C fibers or any sympathetic fibers that innervate vasculature; or 3) Aβ-fibers that innervate Merkel cells. Our use of two antibodies from the same species, and the absence of confocal microscopy for double-labeling leave open the possibility that false positive colocalizations were observed. However, the use of two different H_3R antibodies, and the extensive control procedures employed minimize this possibility.

The present findings strongly support the hypothesis that the H_3R-LI labels the H_3R. All present results were verified with two different antibodies targeted against different domains of the H_3R. Both antibodies labeled CNS regions known to express this receptor (e.g. striatum, cerebral cortex, Pollard et al., 1993). All of the H_3R-LI was eliminated or severely attenuated in H_3R knockout skin, DRGs and CNS. We previously showed that the H_3KO mice used presently lack H_3R radioligand binding, and lack responses to H_3R agonists (Cannon et al., 2003). Although H_3R isoforms may exist (Coge et al., 2001;Wellendorph et al., 2002;Drutel et al., 2001;Tardivel-Lacombe et al., 2000;Rouleau et al., 2004), the H_3KO gene construct eliminated the coding for both antigenic epitopes used presently.

In situ hybridization studies found moderate levels of H_3R mRNA in rat DRGs (Heron et al., 2001), but the characteristics of the positive neurons were not elucidated. Although our methods cannot determine which DRG neurons are the source of particular sensory fibers and endings, the size and immunochemical characteristics of the H_3R-positive neurons are consistent with the caliber and immunochemical characteristics of the H_3R-positive cutaneous innervation. These neurons were primarily medium to large DRG cells that coexpressed NF and CGRP-LI, consistent with our observation that H_3R –LI was expressed on particular types of peptidergic Aδ and Aβ fibers. In contrast, the large neurons that lacked H_3R-LI as well as CGRP-LI are consistent with the characteristics of Aβ fibers that are the source of Merkel endings. Many of the medium size neurons with and without CGRP-LI were also NF-positive, but lacked H_3R-LI. This is consistent with the presence of peptidergic and nonpeptidergic Aδ fibers in the upper dermis that innervate hair follicles and the epidermis (Fundin et al., 1997a;Rice et al., 1997;Fünfschilling et al., 2004). Importantly, most of the small DRG neurons lacked H_3R-LI. These include CGRP-positive and negative neurons that are the source of peptidergic and nonpeptidergic C fibers. Cumulatively, our data indicate that, at least for cutaneous innervation, H_3R functions previously attributed to sensory peptidergic C fibers are most likely to be mediated through peptidergic periarterial Aδ-fiber endings and perhaps Aβ-fiber lanceolate and Meissner endings.

Although functional studies suggest that H_3Rs exist on sympathetic innervation, H_3R-LI was not detected on cutaneous sympathetic NPY-expressing fibers in the rat, and only a few double labeled fibers were seen in the mouse. Some NPY-positive/H_3R-negative neurons were observed in the SCG which could be a source for the sympathetic cutaneous arterial innervation. However, most of the SCG neurons co-expressed H_3R-LI and NPY-LI, implying an H_3R localization on sympathetic neurons. Apparent mismatches between ganglion cell and axon immunochemistry have been noted previously (Fundin et al., 1997a;Rice et al., 1997). The lack of detectable H_3R-LI on the arterial sympathetic fibers may be due to a diffuse distribution among their extensive terminal arborizations. Alternatively, the SCG may contain H_3R-positive sympathetic neurons that innervate structures other than the skin.

Functional roles for the H_3R

H_3R agonists are known to inhibit neuropeptide release from presumed sensory fibers in the heart, lung, and skin. Consistent with this, H_3R agonists have some anti-inflammatory and

antinociceptive properties (Rouleau et al., 1997;Rouleau et al., 2000;Cannon et al., 2003,Cannon and Hough, 2005). The present results show that periarterial Aδ fibers possess the H_3R and are likely to be a site of H_3 agonist action. However, some Aβ fibers, as well as keratinocytes also have both H_3R-LI and CGRP immunoreactivity, and therefore may also have functional signficance.

H_3R antagonists have been reported to produce pruritus-like effects in mice, possibly mediated by C fibers (Schmelz et al., 1997;Hossen et al., 2003;Sugimoto et al., 2004). Because H_3R–LI is present on keratinocytes but not on epidermal endings, the former may participate in these effects of H_3R antagonists. Recently, keratinocytes have been shown to be critical mediators following the activation of endothelin B (Khodorova et al., 2003) and cannabinoid CB_2 receptors (Ibrahim et al., 2005).

Although the lanceolate and Meissner endings that are supplied by H_3R positive Aβ-fibers are thought to be rapidly adapting low threshold mechanoreceptors, the Meissner endings express a wide range of immunochemical properties associated with nociception (Paré et al., 2001). Both types of endings are also intimately affiliated with several types of C fibers (Fundin et al., 1997a; Paré et al., 2001). The functional importance of these chemical characteristics and potential interactions with the affiliated C fibers in the skin have not been investigated. However, modulation of Aβ fiber activity is known to afffect pain sensations that have typically been attributed to C fiber and/or Aδ fiber activity. Peripheral, as well as central mechanisms could account for these observations.

We recently reported that pharmacological activation of spinal H_3Rs inhibits mechanical nociceptive responses to tail pinch in wildtype, but not H_3KO mice (Cannon et al., 2003). This effect is both modality- and intensity- specific (Cannon et al., 2003;Hough and Cannon, 2005). For example, noxious thermal responses are unaffected. The intensity of the mechanical stimulus needed to elicit these responses suggests that the relevant fibers are high threshold mechanoreceptors (HTM) (Burgess and Perl, 1967;Beck et al., 1974;Szolcsanyi et al., 1988;Yeomans and Proudfit, 1996;Ringkamp et al., 2001). Consistent with the spinal H_3R inhibition of mechanical nociception, we detected H_3R-LI on small caliber CGRP-positive fibers ramifying in the superficial laminae of the dorsal horn, as well as in lamina V, which are known sites of HTM termination (Light and Perl, 1979). We hypothesize that these HTMs are the periarterial Aδ fibers. Consistent with this, Aδ HTMs in the deep dermis of guinea pigs were shown to be CGRP-immunoreactive (Lawson et al., 2002). We also found that these periarterial Aδ fibers coexpressed immunoreactivity for ASIC3, a channel which has been implicated in mechanical nociceptive transmission (Price et al., 2001). Conceivably, the high intensity mechanical stimulus needed to activate HTMs and the lack of thermal responsiveness may not be an inherent property of the fiber, but may be due to their relatively deep disposition in the skin. The close proximity of these fibers to blood vessels and their probable mechanosensitivity suggest the possibility that vasodilation could provide local mechanical forces to activate these fibers.

The H_3R-mediated inhibition of neuropeptide release in skin may be an important mechanism to control the extent of inflammation that occurs during or following injury. CGRP and SP, released during tissue damage, produce vasodilation and plasma extravasation (Brain et al., 1992;Brain and Williams, 1989;Lembeck and Holzer, 1979;Saria, 1984), which, in turn, allow the infiltration of additional inflammatory mediators (Bar-Shavit et al., 1980;Hartung et al., 1986;Helme and Andrews, 1985; Payan et al., 1984; Saito et al., 1986). Peptide release also activates mast cells to release histamine (Johnson and Erdos, 1973;Owen et al., 1980;Owen and Woodward, 1980). Subsequent activation of H_1 receptors on nociceptive fibers results in sensitization and increased pain (Mobarakeh et al., 2000;Owen et al., 1980;Owen and Woodward, 1980), but activation of H_3Rs can inhibit further peptide release from such endings

as the periarterial Aδ fibers, thereby limiting subsequent inflammatory events (Dimitriadou et al., 1994;Ohkubo et al., 1995;Delaunois et al., 1995;Imamura et al., 1996;Dimitriadou et al., 1997;Nemmar et al., 1999). Consistent with this, several studies have demonstrated that systemic administration of the H_3R agonist immepip significantly attenuates formalin-induced paw swelling (Imamura et al., 1996; Cannon et al., manuscript submitted). Thus, the injury-induced release of histamine may play a pronociceptive, pro-inflammatory role through H_1 receptors, and/or an anti-inflammatory, antinociceptive role via H_3Rs (Imamura et al., 1996).

Acknowledgements

This work was supported by grants from the National Institute on Drug Abuse (DA-03816, DA-015915, and DA-07307) and the Wellcome Trust (UK). We thank Dr. I. Silos-Santiago formerly of Millennium Pharmaceuticals, Inc. (Cambridge, MA) for providing H_3KO mice.

Reference List

Abercrombie M. Estimation of nuclear population from microtome sections. Anat Rec 1946;94:239–247.

Amann R, Schuligoi R, Holzer P, Donnerer J. The nonpeptide NK1 receptor antagonist Sr140333 produces long lasting inhibition of neurogenic inflammation, but does not influence acute chemonociception or thermonociception in rats. Naunyn-Schmiedebergs Arch Pharmacol 1995;352:201–205. [PubMed: 7477444]

Arrang JM, Garbarg M, Lancelot J, Lecomte JM, Pollard H, Robba M, Schunack W, Schwart JC. Highly potent and selective ligands for histamine H_3-receptors. Nature 1987;327:117–123. [PubMed: 3033516]

Arrang JM, Garbarg M, Schwart JC. Auto-inhibition of brain histamine release mediated by a novel class (H_3) of histamine receptors. Nature 1983;302:832–837. [PubMed: 6188956]

Bar-Shavit Z, Goldman R, Stabinsky Y, Gottlieb P, Fridkin M, Teichberg VI, Blumberg S. Enhancement of phagocytosis—a newly found activity of Substance P residing in its N-terminal tetrapeptide. Biochem Biophys Res Comm 1980;94:1445–1451. [PubMed: 6156684]

Basbaum, AI.; Jessell, TM. The Perception of Pain. In: Kandel, ER.; Schwartz, JH.; Jessell, TM., editors. Principles of Neural Science. New York: McGraw-Hill; 2000. p. 472-491.

Beck PW, Handwerker HO, Zimmermann M. Nervous outflow from the cat's foot during noxious radiant heat stimulation. Brain Res 1974;67:373–386. [PubMed: 4470431]

Brain SD, Cambridge H, Hughes SR, Wilsoncroft P. Evidence that calcitonin gene-related peptide contributes to inflammation in skin and joint. Ann N Y Acad Sci 1992;657:412–419. [PubMed: 1637097]

Brain SD, Williams TJ. Interactions between tachykinins and calcitonin gene-related peptide lead to the modulation of oedema formation and blood flow in rat skin. Br J Pharmacol 1989;97:77–82. [PubMed: 2470460]

Burgess PR, Perl ER. Myelinated afferent fibres responding specifically to noxious stimulation of the skin. J Physiol 1967;190:541–562. [PubMed: 6051786]

Cannon KE, Nalwalk JW, Stadel R, Ge P, Lawson D, Silos-Santiago I, Hough LB. Activation of spinal histamine H_3 receptors inhibits mechanical nociception. Eur J Pharmacol 2003;470:139–147. [PubMed: 12798951]

Cannon KE, Hough LB. Inhibition of chemical and low-intensity mechanical nociception by activation of histamine H_3 receptors. J Pain 2005;6:193–200. [PubMed: 15772913]

Chazot PL, Hann V, Wilson C, Lees G, Thompson CL. Immunological identification of the mammalian H_3 histamine receptor in the mouse brain. Neuroreport 2001;12:259–262. [PubMed: 11209931]

Chen J, Liu C, Lovenberg TW. Molecular and pharmacological characterization of the mouse histamine H(3) receptor. Eur J Pharmacol 2003;467:57–65. [PubMed: 12706455]

Coge F, Guenin SP, Audinot V, Renouard-Try A, Beauverger P, Macia C, Ouvry C, Nagel N, Rique H, Boutin JA, Galizzi JP. Genomic organization and characterization of splice variants of the human histamine H_3 receptor. Biochem J 2001;355:279–288. [PubMed: 11284713]

Delaunois A, Gustin P, Garbarg M, Ansay M. Modulation of acetylcholine, capsaicin and substance P effects by histamine H3 receptors in isolated perfused rabbit lungs. Eur J Pharmacol 1995;277:243–250. [PubMed: 7493615]

Dimitriadou V, Rouleau A, Dam Trung TM, Newlands GJ, Miller HR, Luffau G, Schwartz JC, Garbarg M. Functional relationship between mast cells and C-sensitive nerve fibres evidenced by histamine H3-receptor modulation in rat lung and spleen. Clin Sci (Lond) 1994;87:151–163. [PubMed: 7924160]

Dimitriadou V, Rouleau A, Trung T, Newlands GJ, Miller HR, Luffau G, Schwartz JC, Garbarg M. Functional relationships between sensory nerve fibers and mast cells of dura mater in normal and inflammatory conditions. Neuroscience 1997;77:829–839. [PubMed: 9070755]

Drew LJ, Rohrer DK, Price MP, Blaver KE, Cockayne DA, Cesare P, Wood JN. Acid-sensing ion channels ASIC2 and ASIC3 do not contribute to mechanically activated currents in mammalian sensory neurones. J Physiol 2004;556:691–710. [PubMed: 14990679]

Drutel G, Peitsaro N, Karlstedt K, Wieland K, Smit MJ, Timmerman H, Panula P, Leurs R. Identification of rat H_3 receptor isoforms with different brain expression and signaling properties. Mol Pharmacol 2001;59:1–8. [PubMed: 11125017]

Fitzsimons C, Engel N, Duran H, Policastro L, Cricco G, Martin G, Molinari B, Rivera E. Histamine production in mouse epidermal keratinocytes is regulated during cellular differentiation. Inflamm Res 2001;50:S100–S101. [PubMed: 11411573]

Fundin BT, Arvidsson J, Aldskogius H, Johansson O, Rice SN, Rice FL. Comprehensive immunofluorescence and lectin binding analysis of intervibrissal fur innervation in the mystacial pad of the rat. J Comp Neurol 1997a;385:185–206. [PubMed: 9268123]

Fundin BT, Pfaller K, Rice FL. Different distribution of the sensory and autonomic innervation among the microvasculature of the rat mystacial pad. J Comp Neurol 1997b;389:545–568. [PubMed: 9421138]

Fünfschilling U, Ng Y-G, Zang K, Miyazaki JK, Reichardt LF, Rice FL. TrkC kinase expression in distinct subsets of cutaneous trigeminal innervation and non-neuronal cells. J Comp Neurol 2004;480:392–414. [PubMed: 15558783]

Godlewski G, Malinowska B, Buczko W, Schlicker E. Inhibitory H3 receptors on sympathetic nerves of the pithed rat: activation by endogenous histamine and operation in spontaneously hypertensive rats. Naunyn Schmiedebergs Arch Pharmacol 1997a;355:261–266. [PubMed: 9050021]

Godlewski G, Malinowska B, Schlicker E, Bucher B. Identification of histamine H3 receptors in the tail artery from normotensive and spontaneously hypertensive rats. J Cardiovasc Pharmacol 1997b; 29:801–807. [PubMed: 9234662]

Hartung H-P, Wolters K, Tokya KV. Substance P binding properties and studies on cellular responses in guinea-pig macrophages. J Immunol 1986;136:3856–3863. [PubMed: 2422264]

Helme RD, Andrews PV. The effect of nerve lesions on the inflammatory response to injury. J Neurosci Res 1985;13:453–459. [PubMed: 3921721]

Heron A, Rouleau A, Cochois V, Pillot C, Schwartz JC, Arrang JM. Expression analysis of the histamine H(3) receptor in developing rat tissues. Mech Dev 2001;105:167–173. [PubMed: 11429293]

Hossen MA, Sugimoto Y, Kayasuga R, Kamei C. Involvement of histamine H3 receptors in scratching behaviour in mast cell-deficient mice. Br J Dermatol 2003;149:17–22. [PubMed: 12890190]

Hough LB. Genomics Meets Histamine Receptors: New Subtypes, New Receptors. Mol Pharmacol 2001;59:1–5. [PubMed: 11125017]

Hough, LB.; Leurs, R. Histamine. In: Siegel, G.; Agranoff, B.; Albers, R.; Fisher, S.; Uhler, M., editors. Basic Neurochemistry. 7. Lippincott: Williams and Wilkins; 2006. p. 249-266.

Ibrahim MM, Porreca F, Lai J, Albrecht PJ, Rice FL, Khodorova A, Davar G, Makriyannis A, Vanderah TW, Mata HP, Malan TP Jr. CB_2 cannabinoid receptor activation produces antinociception by stimulating peripheral release of endogenous opioids. Proc Natl Acad Sci USA 2005;102:3093–3098. [PubMed: 15705714]

Imamura M, Smith NC, Garbarg M, Levi R. Histamine H_3-receptor-mediated inhibition of calcitonin gene-related peptide release from cardiac C fibers. A regulatory negative-feedback loop. Circ Res 1996;78:863–869. [PubMed: 8620607]

Ishikawa S, Sperelakis N. A novel class (H3) of histamine receptors on perivascular nerve terminals. Nature 1987;327:158–160. [PubMed: 3033517]

Johnson AR, Erdos EG. Release of histamine from mast cells by vasoactive peptides. Proc Soc Exp Biol Med 1973;142:1252–1256. [PubMed: 4121082]

Karlstedt K, Ahman MJ, Anichtchik OV, Soinila S, Panula P. Expression of the H_3 eceptor in the developing CNS and brown fat suggests novel roles for histamine. Mol Cell Neurosci 2003;24:614–622. [PubMed: 14664812]

Khodorova A, Navarro B, Jouaville LS, Murphy JE, Rice FL, Mazurkiewicz JE, Long-Woodward D, Stoffel M, Strichartz GR, Yukhananov R, Davar G. Endothelin-B receptor activation triggers an endogenous analgesic cascade at sites of peripheral injury. Nat Med 2003;9:1055–1061. [PubMed: 12847519]

Koss MC. Histamine H_3 receptor activation inhibits sympathetic-cholinergic responses in cats. Eur J Pharmacol 1994;257:109–115. [PubMed: 8082690]

Lawson SN, Crepps B, Perl ER. Calcitonin gene-related peptide immunoreactivity and afferent receptive properties of dorsal root ganglion neurones in guinea-pigs. J Physiol 2002;540:989–1002. [PubMed: 11986384]

Lembeck F, Holzer P. Substance P as neurogenic mediator of antidromic vasodilation and neurogenic plasma extravasation. Naunyn Schmiedebergs Arch Pharmacol 1979;352:201–205.

Light AR, Perl ER. Spinal termination of functionally identified primary afferent neurons with slowly conducting myelinated fibers. J Comp Neurol 1979;186:133–150. [PubMed: 109477]

Lovenberg TW, Roland BL, Wilson SJ, Jiang X, Pyati J, Huvar A, Jackson MR, Erlander MG. Cloning and functional expression of the human histamine H_3 receptor. Mol Pharmacol 1999;55:1101–1107. [PubMed: 10347254]

McCarthy PW, Lawson SN. Cell type and conduction velocity of rat primary sensory neurons with calcitonin gene-related peptide-like immunoreactivity. Neuroscience 1990;34:623–32. [PubMed: 2352644]

Millan MJ. The induction of pain: an integrative review. Prog Neurobiol 1999;57:1–164. [PubMed: 9987804]

Mobarakeh JI, Nalwalk JW, Watanabe T, Sakurada S, Hoffmann M, Leurs R, Timmerman H, Silos-Santiago I, Yanai K, Hough LB. Improgan antinociception does not require neuronal histamine or histamine receptors. Brain Res 2003;974:146–152. [PubMed: 12742632]

Mobarakeh JI, Sakurada S, Katsuyama S, Kutsuwa M, Kuramasu A, Lin ZY, Watanabe T, Hashimoto Y, Yanai K. Role of histamine H(1) receptor in pain perception: a study of the receptor gene knockout mice. Eur J Pharmacol 2000;391:81–89. [PubMed: 10720638]

Molderings GJ, Weissenborn G, Schlicker E, Likungu J, Gothert M. Inhibition of noradrenaline release from the sympathetic nerves of the human saphenous vein by presynaptic histamine H3 receptors. Naunyn Schmiedebergs Arch Pharmacol 1992;346:46–50. [PubMed: 1328894]

Molliver DC, Immke DC, Fierro L, Pare M, Rice FL, McCleskey EW. ASIC3, an acid-sensing ion channel, is expressed in metaboreceptive sensory neurons. Molecular Pain 2005 2004;1:35.

Nemmar A, Delaunois A, Beckers JF, Sulon J, Bloden S, Gustin P. Modulatory effect of imetit, a histamine H3 receptor agonist, on C-fibers, cholinergic fibers and mast cells in rabbit lungs in vitro. Eur J Pharmacol 1999;371:23–30. [PubMed: 10355590]

Ohkubo T, Shibata M, Inoue M, Kaya H, Takahashi H. Regulation of substance P release mediated via prejunctional histamine H_3 receptors. Eur J Pharmacol 1995;273:83–88. [PubMed: 7537682]

Owen DA, Poy E, Woodward DF, Daniel D. Evaluation of the role of histamine H_1- and H_2- receptors in cutaneous inflammation in the guinea-pig produced by histamine and mast cell degranulation. Br J Pharmacol 1980;69:615–623. [PubMed: 6108140]

Owen DA, Woodward DF. Histamine and histamine H_1- and H_2-receptor antagonists in acute inflammation. Biochem Soc Trans 1980;8:150–155. [PubMed: 6102933]

Pare M, Smith AM, Rice FL. Distribution and terminal arborizations of cutaneous mechanoreceptors in the glabrous finger pads of the monkey. J Comp Neurol 2002;445:347–359. [PubMed: 11920712]

Pillot C, Heron A, Cochois V, Tardivel-Lacombe J, Ligneau X, Schwartz JC, Arrang JM. A detailed mapping of the histamine H(3) receptor and its gene transcripts in rat brain. Neuroscience 2002;114:173–193. [PubMed: 12207964]

Pollard H, Moreau J, Arrang JM, Schwartz JC. A detailed autoradiographic mapping of histamine H_3 receptors in rat brain areas. Neuroscience 1993;52:169–189. [PubMed: 8381924]

Price MP, McIlwrath SL, Xie J, Cheng C, Qiao J, Tarr DE, Sluka KA, Brennan TJ, Lewin GR, Welsh MJ. The DRASIC cation channel contributes to the detection of cutaneous touch and acid stimuli in mice. Neuron 2001;32:1071–1083. [PubMed: 11754838]

Rice FL, Fundin BT, Arvidsson J, Aldskogius H, Johansson O. Comprehensive immunofluorescence and lectin binding analysis of vibrissal follicle sinus complex innervation in the mystacial pad of the rat. J Comp Neurol 1997;385:149–184. [PubMed: 9268122]

Rice FL, Albers KM, Davis BM, Silos-Santiago I, Wilkinson GA, LeMaster AM, Ernfors PJ, Smeyne RJ, Aldskogius H, Phillips HS, Barbacid M, DeChiara TM, Yancopoulos GD, Dunne CE, Fundin BT. Differential effects of various neurotrophin and trk receptor deletions on the unmyelinated innervation of the epidermis in the whisker pad of the mouse. Develop Biol 1998;198:57–81. [PubMed: 9640332]

Rice FL, Rasmusson DD. Innervation of the digit on the forepaw of the raccoon. J Comp Neurol 2000;417:467–490. [PubMed: 10701867]

Ringkamp M, Peng YB, Wu G, Hartke TV, Campbell JN, Meyer RA. Capsaicin responses in heat-sensitive and heat-insensitive A-fiber nociceptors. J Neurosci 2001;21:4460–4468. [PubMed: 11404433]

Rouleau A, Garbarg M, Ligneau X, Mantion C, Lavie P, Advenier C, Lecomte JM, Krause M, Stark H, Schunack W, Schwartz JC. Bioavailability, antinociceptive and antiinflammatory properties of BP 2-94, a histamine H_3 receptor agonist prodrug. J Pharmacol Exp Ther 1997;281:1085–1094. [PubMed: 9190840]

Rouleau A, Heron A, Cochois V, Pillot C, Schwartz JC, Arrang JM. Cloning and expression of the mouse histamine H_3 receptor: evidence for multiple isoforms. J Neurochem 2004;90:1331–1338. [PubMed: 15341517]

Rouleau A, Stark H, Schunack W, Schwartz JC. Anti-inflammatory and antinociceptive properties of BP 2-94, a histamine H(3)-receptor agonist prodrug. J Pharmacol Exp Ther 2000;295:219–225. [PubMed: 10991982]

Saito A, Kimura S, Goto K. Calcitonin gene-related peptide as potential neurotransmitter in guinea-pig right atrium. Am J Physiol 1986;250:H693–698. [PubMed: 2870646]

Saria A. Substance P in sensory nerve fibers contributes to the development of oedema in the rat hindpaw after thermal injury. Br J Pharmacol 1984;323:341–342.

Schmelz M, Schmidt R, Bickel A, Handwerker HO, Torebjork HE. Specific C-receptors for itch in human skin. J Neurosci 1997;17:8003–8008. [PubMed: 9315918]

Shenton FC, Hann V, Chazot PL. Evidence for native and cloned H3 histamine receptor higher oligomers. Inflammation Res 2005;54(Suppl 1):548–549.

Sugimoto Y, Iba Y, Nakamura Y, Kayasuga R, Kamei C. Pruritus-associated response mediated by cutaneous histamine H3 receptors. Clin Exp Allergy 2004;34:456–459. [PubMed: 15005741]

Szolcsanyi J, Anton F, Reeh PW, Handwerker HO. Selective excitation by capsaicin of mechano-heat sensitive nociceptors in rat skin. Brain Res 1988;446:262–268. [PubMed: 3370489]

Tardivel-Lacombe J, Rouleau A, Heron A, Morisset S, Pillot C, Cochois V, Schwartz JC, Arrang JM. Cloning and cerebral expression of the guinea pig histamine H3 receptor: evidence for two isoforms. Neuroreport 2000;11:755–759. [PubMed: 10757514]

Wellendorph P, Goodman MW, Burstein ES, Nash NR, Brann MR, Weiner DM. Molecular cloning and pharmacology of functionally distinct isoforms of the human histamine H(3) receptor. Neuropharmacology 2002;42:929–940. [PubMed: 12069903]

Yeomans DC, Proudfit HK. Nociceptive responses to high and low rates of noxious cutaneous heating are mediated by different nociceptors in the rat: electrophysiological evidence. Pain 1996;68:141–150. [PubMed: 9252009]

Zylka MJ, Rice FL, Anderson DJ. Axonal tracers targeted to *Mrgprd* define a nociceptive circuit with exclusive peripheral projections to the epidermis. Neuron 2005;45:17–25. [PubMed: 15629699]

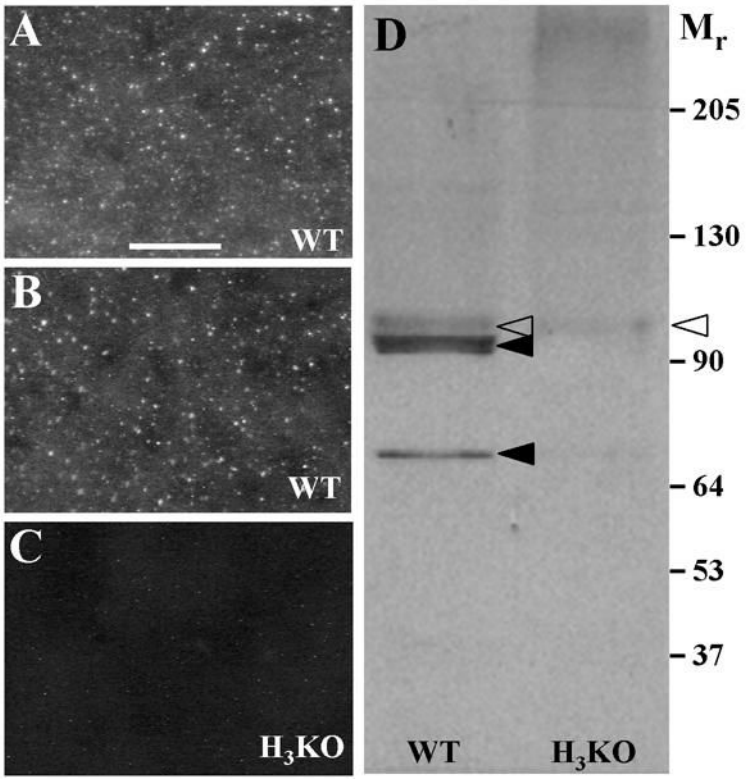

Figure 1. Characterization of anti H_3R labeling

A–C. Digital images of punctate anti-H_3R labeling among the neurons in the striatum as seen in coronal sections from wildtype (A, B) and H_3KO mice (C). Scale bar, 25 μm. Comparable labeling was obtained with anti-H_3R antibodies produced independently by Chazot et al. (2001) (A) and Chemicon (B). Virtually all labeling is absent in the striatum of H_3KO mice prepared with the Chazot antibody (C). D. A Western blot with the Chazot antibody reveals two dense bands (solid arrowheads) in the wildtype mice that are eliminated in H_3KO mice, and a faint band (open arrowheads) that is reduced but still persists in the H_3KO mice.

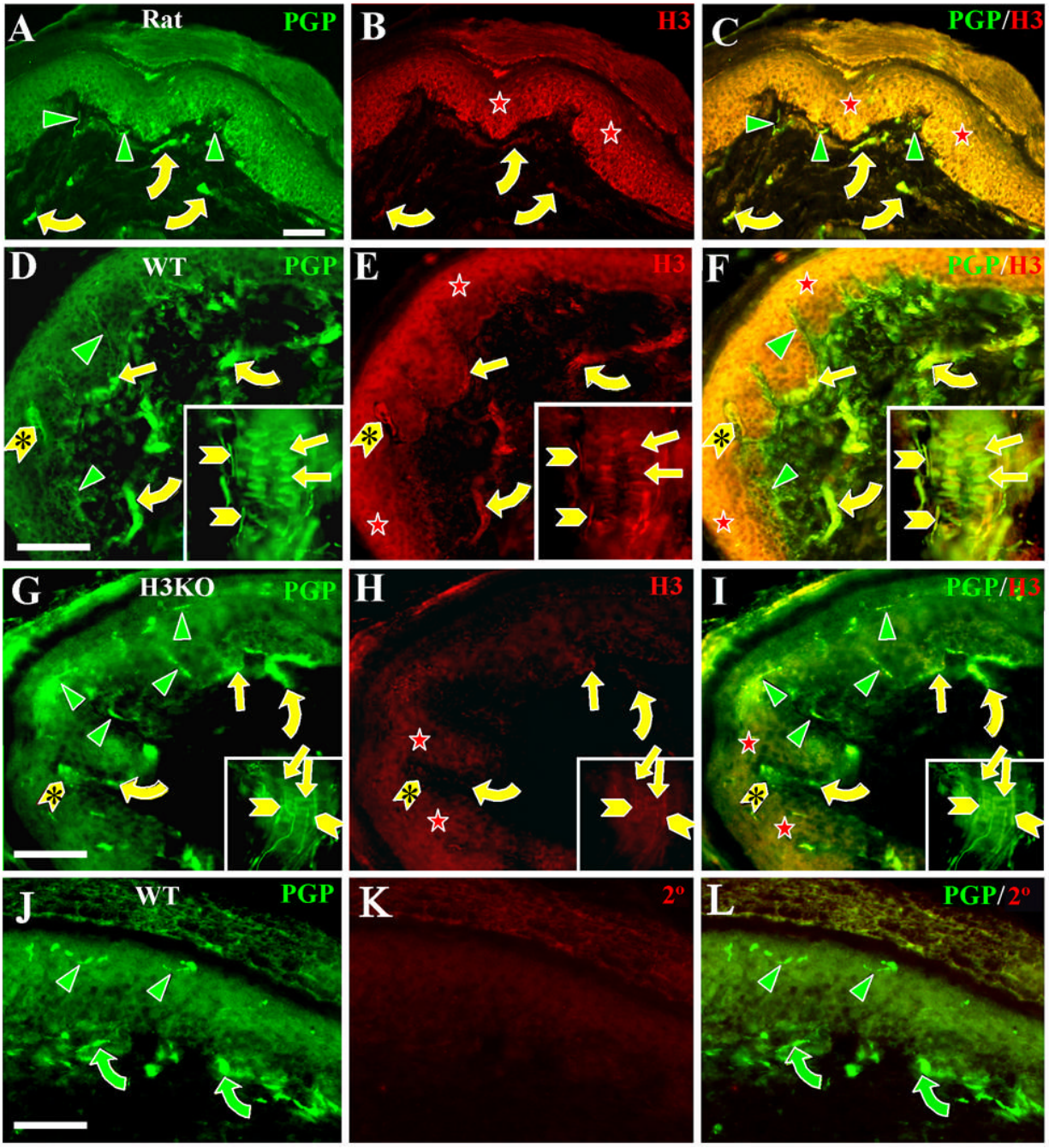

Figure 2. H_3R -LI is absent on thin caliber innervation to the epidermis and upper dermis, but is present on some Aβ fiber innervation, Merkel cells and keratinocytes

Digital images of glabrous hind paw sections from rats (A–C), wild type mice (D–F, J–L), and H_3KO (G–I) mice double labeled with anti-PGP (left panels) and anti-H_3R (middle panels). Merged double labeled images are shown in the right panels. Insets in D–I show labeling in whisker follicles from mystacial pads. Scale bars = 25 μm (50μm for insets). In this and subsequent figures, green (Cy2 or Alexa 488) and red (Cy3) symbols indicate single labeled structures; yellow symbols indicate double labeled structures. A–F: As seen in rat and wildtype mouse skin, thin caliber innervation labeled with anti-PGP (green arrowheads) in the epidermis or upper dermis is not labeled with anti-H_3R. This includes all C-fiber and Aδ-fiber innervation.

Anti-PGP and anti-H_3R double labeling was present on some large caliber Aβ fibers (yellow curved arrows), and on Aβ-fiber endings in Meissner corpuscles (yellow chevrons with asterisks) and Aβ-fiber endings on whisker follicles (yellow chevrons) and hair follicles (not shown). H_3R-LI is also present on keratinocytes in the epidermis (red stars) as well as on anti-PGP labeled Merkel cells (yellow straight arrows) in lamina basalis of the epidermis and the outer root sheath of whisker follicles. H_3R-LI was not evident on the Aβ fibers that innervate the Merkel cells. G–I: In H_3KO mice, H_3R-LI is drastically reduced but faint residual Cy3 labeling was detected on keratinocytes in the epidermis (red stars), some Aβ fibers (yellow curved arrows), Meissner corpuscles (yellow chevrons with arrowheads), lanceolate endings (yellow chevrons) and Merkel cells (yellow straight arrows). All thin caliber innervation was Cy3 negative (green arrowheads). J–L. Images of wildtype glabrous mouse skin double labeled with anti-PGP and peptide preabsorbed anti-H_3R. None of the innervation (green arrowheads and curved arrows) nor cells in the epidermis were labeled with the preabsorbed anti-H_3R.

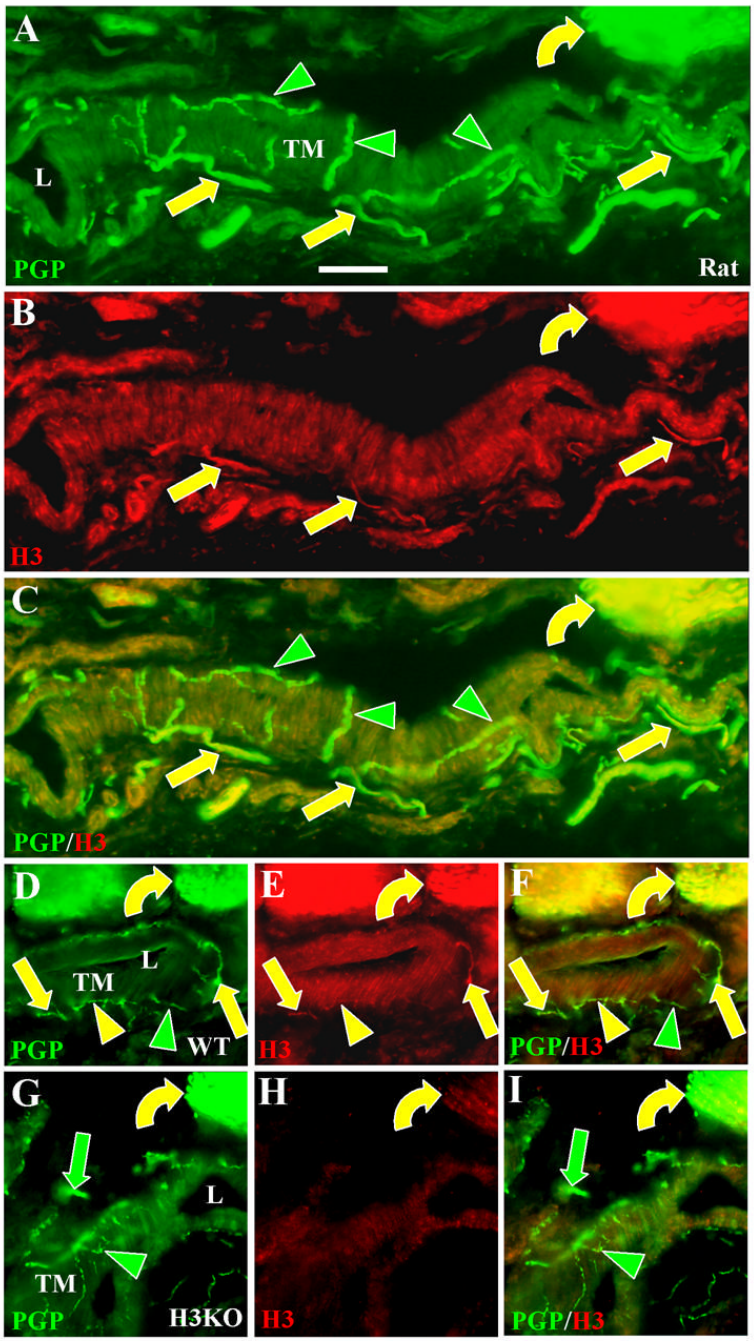

Figure 3. H_3R-LI on periarterial innervation in the deep dermis

Digital images of glabrous hind paw sections from rats (A–C), wildtype mice (D–F), and H_3KO mice (G–I) double labeled with anti-PGP (A, D, G) and anti H_3R revealed with Cy3 (B, E, H). Scale bars, 25 μm. L = arterial lumens, TM = tunica media. A–F. Double labeling is present among individual axons and bundles of axons (yellow straight arrows) which are located in the tunica adventitia (which surrounds the tunica media) and have previously been shown to be mostly CGRP-positive presumptive C fibers and Aδ fibers (see also Fig. 4). Thin-caliber fibers that ramify at the interface between the tunica adventitia and tunica media have previously been shown to be NPY and TH-positive and are presumptive sympathetic innervation. They were entirely labeled only with anti-PGP (green arrowheads) in the rat, but

some double labeled with anti-H_3R in the mouse (yellow arrowheads). Many Aβ fibers in large deep dermal nerves were double labeled (yellow curved arrows). G–I. No H_3R-LI was present among sensory (green arrows) and sympathetic (green arrowheads) periarterial fibers in H_3KO mice, but faint residual labeling was detected on Aβ fibers (yellow curved arrows).

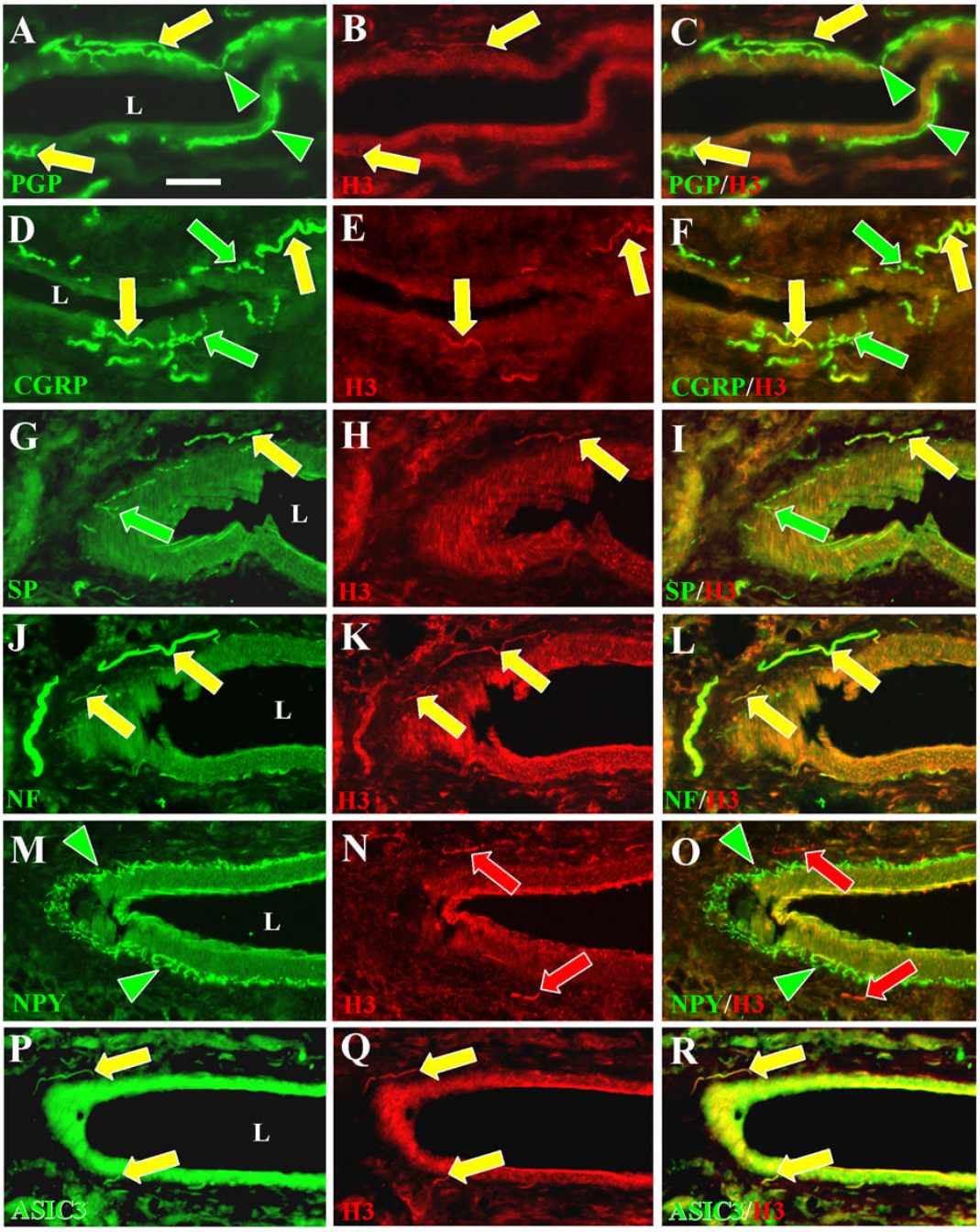

Figure 4. Co-localization of H_3 receptors with CGRP, SP, NF, and ASIC3, but not NPY on deep dermal, peptidergic, arterial innervation

Digital images of glabrous hind paw sections from rats double labeled with antibodies against H_3R (middle panels) and against several other neuronal antigens (left panels). Merged images are in the right panels. The Chemicon anti-H_3R used in B (yellow arrows) did not label innervation as intensely as the Chazot antibody used in all the other middle panels (red and yellow arrows). Scale bar, 25 μm. L = lumen of arteries. A–C. H_3R-LI was expressed almost entirely among the anti-PGP individual fibers and bundles of fibers (yellow arrows) located in the tunica adventitia which surrounds the tunica media. Anti-PGP labeled fibers that ramify at the interface between the tunica adventitia and tunica media lack H_3R-LI (green arrowheads).

D–F. CGRP-LI was expressed in the periarterial innervation that is presumably sensory (yellow and green arrows). A subset of this innervation co-expresses H_3R–LI (yellow arrows). G–I. SP-LI was also expressed in periarterial fibers that are presumably sensory (yellow and green arrows). H_3R-LI was expressed on a subset of this innervation (yellow arrows). J–L. H_3R–LI was expressed on periarterial fibers that co-labeled with anti-NF. Previous studies showed that the NF-positive fibers are a subset of those that label with anti-CGRP. M–O. H_3R-LI was only expressed on fibers (red arrows) that were distinct from those that label with anti-NPY (green arrowheads). P–R. H_3R-positive fibers also labeled with anti-ASIC3 (yellow arrows).

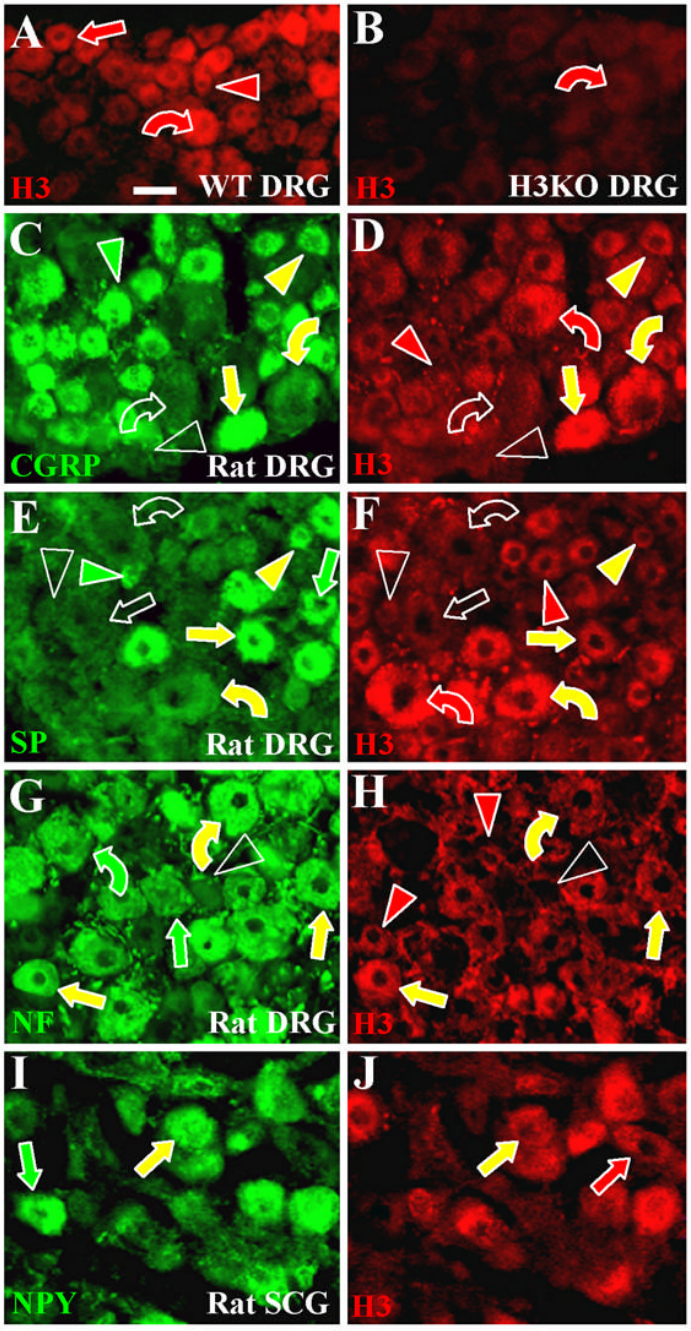

Figure 5. Immunochemical characterization of H_3R expressing neurons in lumbar dorsal root ganglia (DRG) and superior cervical ganglia (SCG)

Sections of ganglia were all labeled with anti-H_3R (red) and some sections were double labeled with another antibodies (green). Small size neurons are indicated by arrowheads, medium size neurons by straight arrows and large size neurons by curved arrows. Red indicators show neurons only labeled with anti-H_3R, green indicators only neurons labeled with other antibodies, and yellow indicators neurons that are double labeled. Empty indicators show neurons that were regarded as having only background fluorescence. Scale bar = 25μm. A, B. Images from mouse DRG sections. Anti-H_3R labeled many of the small (red arrowhead), medium (red arrow) and large (red curved arrow) DRG neurons from a wildtype mouse (A).

Anti-H_3R is virtually eliminated in DRG neurons from a H_3KO mouse (B) except for very low residual leveling on some relatively large neurons (red curved arrow). C–H. Images from rat lumbar DRG sections. C, D. Small neurons double labeled with anti-CGRP and anti-H_3R (yellow arrowheads), only labeled with anti-CGRP (green arrowhead), or only labeled with anti-H_3R (red arrowhead). Some small neurons were not labeled with either antibody (unfilled arrowheads). Most medium size neurons expressed both CGRP-IR and H_3R-IR (yellow straight arrows). Large neurons were typically immunolabeled for both CGRP and H_3R (yellow curved arrows) or were negative for both (unfilled curved arrows). E, F. Overall, fewer neurons label with anti-SP than with anti-CGRP. Some small neurons were double labeled with anti-SP and anti-H_3R (yellow arrowheads), only labeled with anti-SP (green arrowhead), or only labeled with anti-H_3R (red arrowhead). Some small neurons were not labeled with either antibody (unfilled arrowheads). Most medium size neurons were immunolabeled for both SP and H_3R (yellow arrows) or negative for both (unfilled arrow). The green straight arrow indicates a relatively rare medium size neuron that only expressed SP-IR. Some large neurons were double labeled with anti-SP and anti-H_3R (yellow curved arrows), some were labeled only with anti-H_3R (red curved arrow), and others were not labeled with either antibody (unfilled curved arrows). G, H. Virtually all small neurons were NF-negative, whereas virtually all medium and large neurons were NF-positive. Small neurons were H_3R-positive (red arrowheads) or negative (unfilled arrowheads). Medium and large neurons were H_3R-positive (yellow straight arrows and curved arrows) or H_3R -negative (green straight arrows and curved arrows). I, J. Double labeling of rat superior cervical ganglia revealed neurons that coexpressed anti-NPY-IR and anti-H_3-IR (yellow arrows) or that are positive only for NPY (green arrow) or H_3R (red arrow).

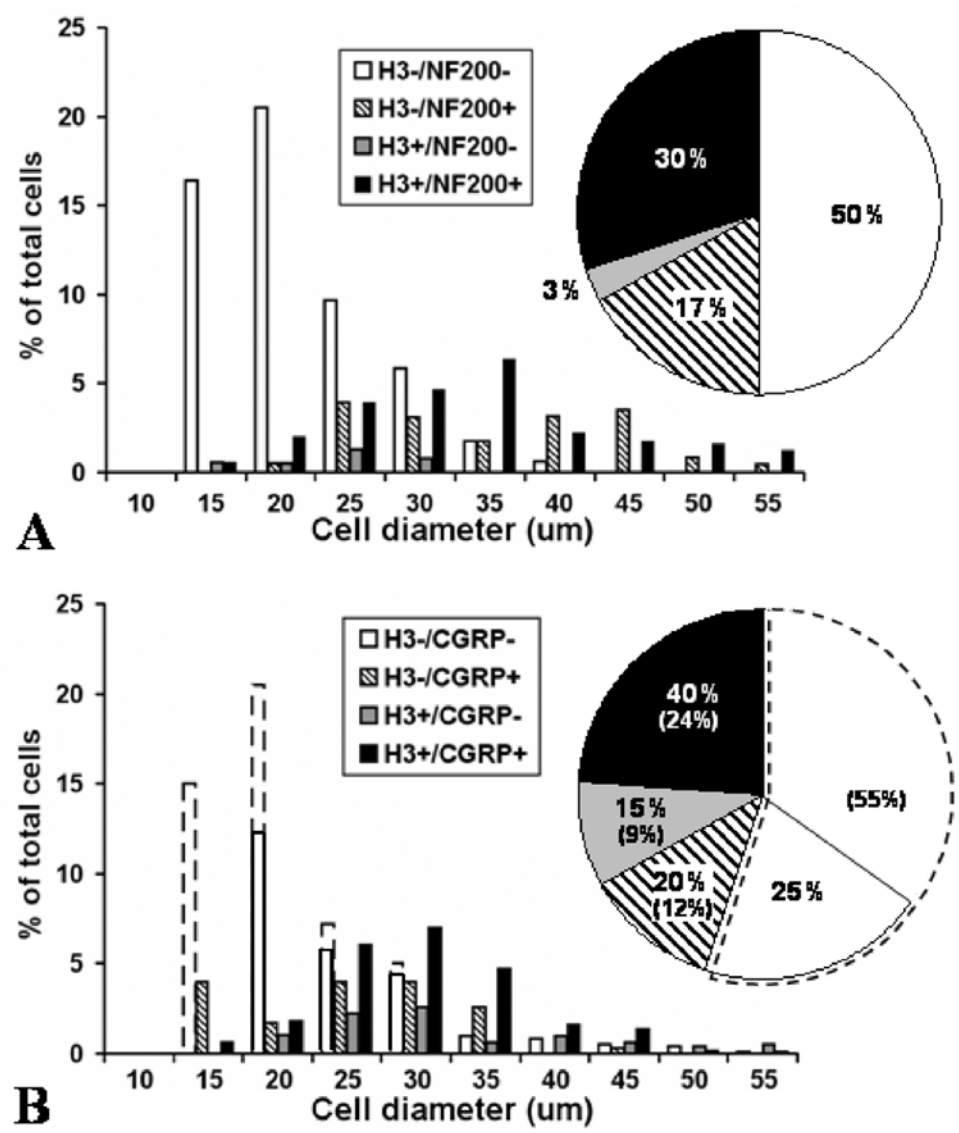

Figure 6. Quantification of anti-H_3R labeling in rat dorsal root ganglia

Distribution of cell sizes and labeling characteristics in rat lumbar DRG neurons as assessed in sections double labeled with anti-H_3R and anti-NF (A) or with anti-H_3R and anti-CGRP (B). Data were normalized from measurements of 758 cells in three L4 and L5 rat DRGs and the proportions were corrected for cell size. A. After double labeling with anti-H_3R and anti-NF, 33% of all presumptive neurons had H_3R–LI. Most of these H_3R–LI neurons were NF-positive (30% vs. 3%) and had medium to large diameters. 17% of all detected neurons were NF-positive and H_3R-negative and had a bimodal distribution among medium and large cells. 50% of presumptive neurons were negative for both H_3R-LI and NF-LI, and most had relatively small diameters. B. After double labeling with anti-H_3R and anti-CGRP, the actual detected proportions of H_3R-positive and negative neurons are shown in the solid line enclosed bars and pie chart sectors. The actual percentages of double-labeled, single-labeled and unlabeled neurons are shown by the numbers without brackets in the pie chart sectors. The proportion of anti-H_3R labeled neurons in B was much higher (55%) than in A (33%), but presumably should be the same. This was most likely due to a failure to detect many unlabeled cells in the anti-H_3R and anti-CGRP labeled sections (see Methods and Results). To correct for this likely lack

of detection, the total % of H_3R–LI neurons observed in the anti-H_3R and anti-CGRP (B) was normalized to 33% by adjusting the proportion of H_3R-negative/CGRP-negative cells to reflect the level of H_3R-negative neurons observed in the anti-H_3R and anti-NF labeled sections (A). The adjusted increase is indicated by broken line bars and pie sectors, and the adjusted percentages are the numbers shown in brackets in B. With or without this adjustment, neurons with H_3R–LI had predominantly medium to large diameters, with a 3:1 ratio of CGRP-positive to CGRP-negative neurons (24% vs 9% in adjusted percentages). Based on adjusted percentages, 12% of the neurons were H_3R-negative and CGRP-positive and had a bimodal distribution among small and medium diameters. Even without an adjustment, the neurons that lacked both H_3R–LI and CGRP-LI were skewed towards smaller diameters (white bars and white pie sector within solid lines).

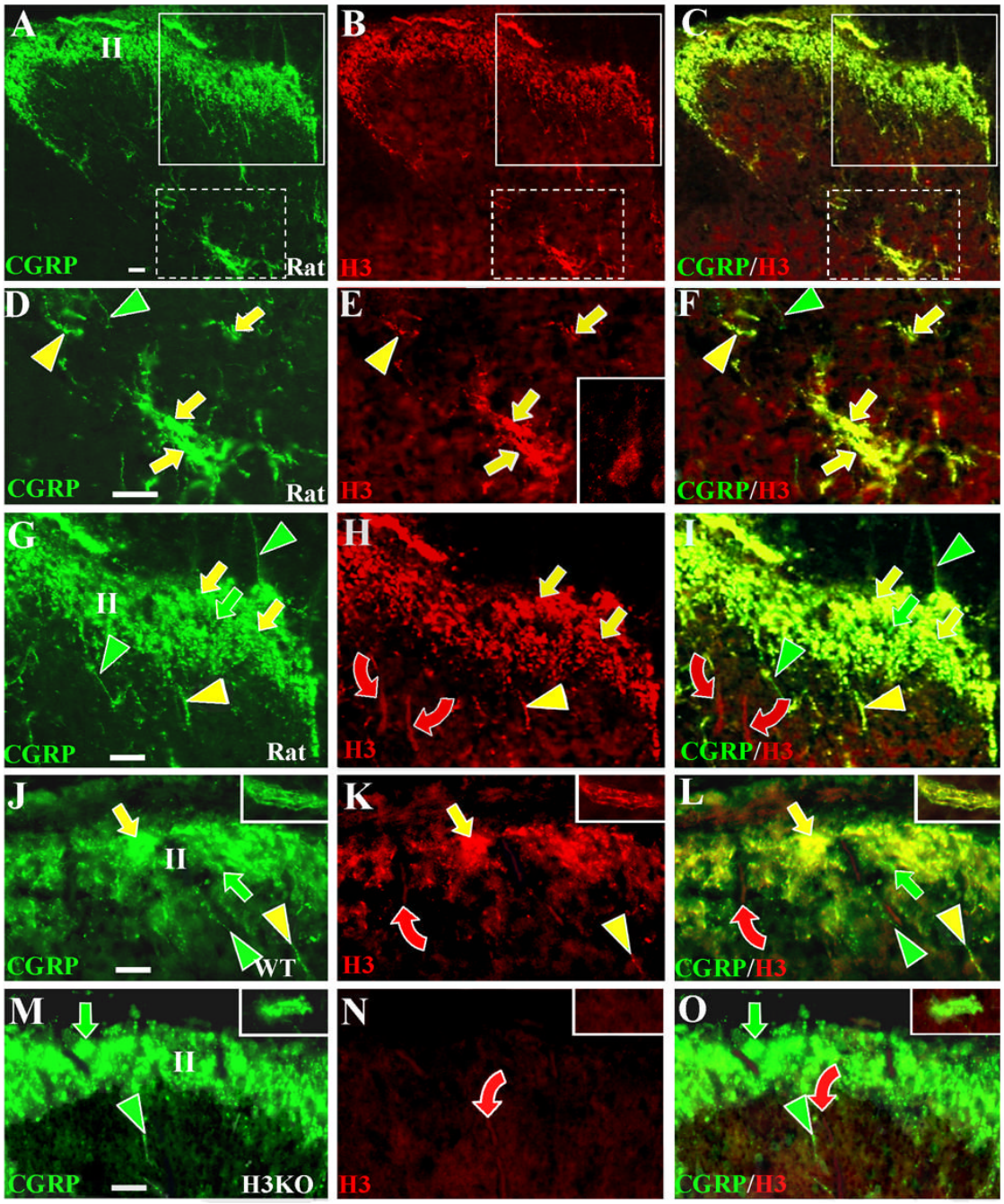

Figure 7. Anti-H_3R labeling in the dorsal horn of rats, wild type mice, and H_3KO mice

Digital cross sectional images of lumbar spinal cords from rats (A–I), wild type mice (J–L), and H_3KO (M–O) mice. The sections are double labeled with anti-CGRP revealed by Cy2 or Alexa 488 conjugated secondary antibodies (left panels) and with the Chazot anti-H_3R revealed by Cy3 conjugated antibodies (middle panels). Merged images are shown in the right panels. Fibers definitively labeled with only anti-CGRP are denoted by green indicators; with only anti-H_3R by red indicators, and with both antibodies by yellow indicators. Scale bars, 25μm. Anti-CGRP and anti-H_3R labeling is shown at low magnification in the rat dorsal horn (A–C). Areas in A–C that include lamina V (white broken line boxes) and laminae I-III (white solid line boxes) are shown at higher magnification in D–F and G–I respectively. Comparable high

magnification images of the superficial dorsal horn are shown for WT (J–L) and H_3KO (M–O) mice. High magnification images from lamina V of mice are shown in insets in J–O. As shown in D–F and in the insets in J–L, most of the CGRP-positive fibers that ramify in lamina V coexpress H_3LI (yellow arrows), whereas few fibers only express CGRP-LI (green arrowheads). As shown in the inset in E, some dorsal horn neurons deep to lamina II have faint levels of H_3R-LI detectable primarily over the cell body. As shown in G–L, anti-CGRP labeled fibers ramify extensively in superficial lamina and include fibers that express H_3R-LI (yellow arrows) and those that lack H_3R-LI (green arrows). Some individual CGRP-positive fibers express H_3R-LI (yellow arrowheads) and others lack H_3R-LI (green arrowheads). Some thick-caliber Aβ fibers passing through the superficial laminae have low levels of H_3R-LI (red curved arrows). As seen in M-O, H_3R-LI is absent on the CGRP-positive innervation in H_3KO mice (green arrows and arrowheads), but very faint residual labeling persists on some Aβ fibers (red curved arrows).

Table 1

List of Antibodies Used for Immunofluorescence Studies

Antigen	Antibody (dilution)	Source
Protein gene product 9.5 PGP)	Rabbit polyclonal (1:800)	UltraClone Ltd. (Wellow, Isle of Wight, UK)
Calcitonin gene-related peptide (CGRP)	Guinea pig polyclonal (1:400)	Peninsula Laboratories Inc. (San Carlos, CA)
Neurofilament 200kD (NF)	Rabbit polyclonal (1:800)	Chemicon International Inc. (Temecula, CA)
Substance P (SP)	Guinea pig polyclonal (1:400)	Research Diagnostics Inc. (Flanders NJ)
Neuropeptide Y (NPY)	Sheep polyclonal (1:800)	Chemicon International Inc.
Acid-sensing ion channel 3(ASIC3)	Guinea Pig (1:500)	Neuromics Antibodies Northfield, MN)
Histamine H_3 receptor (H_3R):		
1) Intracellular loop 3[1] rat and human)	Rabbit polyclonal (1:50–500)	Chazot et al., 2001
2) C-terminus[2] (rat)	Rabbit polyclonal (1:50–500)	Chemicon International Inc.

[1] This antibody was raised against a 10 amino acid peptide sequence found in intracellular loop 3 of the rat and human H_3R protein.

[2] This commercial antibody was raised against the C-terminus of rat H_3R.